

RSC Advances



This is an *Accepted Manuscript*, which has been through the Royal Society of Chemistry peer review process and has been accepted for publication.

Accepted Manuscripts are published online shortly after acceptance, before technical editing, formatting and proof reading. Using this free service, authors can make their results available to the community, in citable form, before we publish the edited article. This *Accepted Manuscript* will be replaced by the edited, formatted and paginated article as soon as this is available.

You can find more information about *Accepted Manuscripts* in the [Information for Authors](#).

Please note that technical editing may introduce minor changes to the text and/or graphics, which may alter content. The journal's standard [Terms & Conditions](#) and the [Ethical guidelines](#) still apply. In no event shall the Royal Society of Chemistry be held responsible for any errors or omissions in this *Accepted Manuscript* or any consequences arising from the use of any information it contains.

Title:

Ultrahigh Rhodamin B adsorption capacities from aqueous solution by activated carbon derived from *Phragmites australis* doped with organic acid by phosphoric acid activation

Author names:

Zizhang Guo, Jian Zhang*, Hai Liu

Author affiliations:

School of Environmental Science and Engineering, Shandong Key Laboratory of Water Pollution Control and Resource Reuse, Shandong University, Jinan 250100, China

*** Corresponding author:**

Tel.: + 86 531 88363015;

Fax: + 86 531 88364513

E-mail address: sdguozizhang@gmail.com; zhangjian00@sdu.edu.cn

Abstract

This work present that oxalic acid (OA) and succinic acid (SA) were employed to modify *Phragmites australis* (PA)-based activated carbons (ACs) during phosphoric acid activation for improving its Rhodamin B (RhB) removal from aqueous solutions. The unmodified activated carbon (AC), OA-modified and SA-modified activated carbon (AC-OA and AC-SA) were characterized by N₂ adsorption/desorption, Boehm's titration, pH_{zpc} and FTIR analysis. It was found that the BET surface area of AC-OA (1040.36 m²/g) and AC-SA (1775.01 m²/g) was larger than AC (745.68 m²/g). In addition, AC-OA (2.987 mmol/g) and AC-SA (3.194 mmol/g) exhibited dramatically higher surface acidic than AC (1.852 mmol/g). The RhB adsorption capacities of ACs were further investigated at different contact times, pHs, and ionic strengths. The adsorption equilibrium data of ACs were properly fitted to the Langmuir model. The kinetic studies show that the adsorption of RhB proceeds according to the pseudo-second order. The maximum RhB adsorption capacities of AC-OA (550.9 mg/g) and AC-SA (629.8 mg/g) were significantly higher than that of AC (417.1 mg/g), resulting from that their larger BET surface areas and higher surface acidic functional groups could attribute RhB adsorption.

Keywords: Activated carbon; Oxalic acid; Succinic acid; Rhodamin B adsorption.

1. Introduction

Synthetic dyes are generally released into the environment from industrial effluents and the discharge of highly colored synthetic dye effluents can be very damaging to the receiving water bodies.¹ Rhodamine B (RhB) is a basic synthetic dye imparting a red color in the aqueous solution and is widely used in paper, textile, leather, and paint industries.² Human being and animal exposure to RhB cause irritation to the skin, eyes and respiratory tract. The carcinogenicity, reproductive and developmental toxicity, neurotoxicity and chronic toxicity of RhB towards humans and animals have been reported.³⁻⁶ What is more, water soluble dyes are characterized by their poor biodegradability and it is estimated that about 20% of the total dye remain in the effluent during the production process, thus, building high concentrations in wastewaters.^{7,8} High concentration of synthetic dyes in the effluents results in the formation of wastewaters characterized by their toxicity, reduced transparency of light and high content of organic load.⁸

Consequently, removal of color synthetic dyestuff from waste effluents becomes environmentally important. Many treatment processes have been applied for the removal of dyes from wastewater, including adsorption,¹ photocatalytic degradation,⁶ chemical oxidation,⁴ electrochemical degradation,⁹ and AOP.¹⁰ Nevertheless, adsorption process using suitable adsorbent has shown high efficiency for removal of dyes. Many adsorbents have been used to remove dyes from wastewater, including tea leaves,¹ industrial solid waste,³ fly ash,⁴ and Fe₃O₄ nanoparticles.⁵ However, their low removal abilities for high concentration dyes

wastewater often limit their application. Activated carbon (AC) is the most widespread adsorbent used in removal of dyes due to its superior removal abilities and adsorption capacities. There are numerous reports on the adsorption removal of RhB with ACs.^{3,11-13} However, the study on the *Phragmites australis* (PA)-based ACs as adsorbent for high concentration of RhB removal from water has not been reported.

A variety of carbonaceous materials such as biomass and their wastes,^{14,15} coal,¹⁶ and some polymers¹⁷ have been used as precursors to prepare ACs. Resulting from the advantages of environmental protection and low-cost, preparing ACs with biomass wastes (lotus stalks, feather, bamboo, etc.) has more and more attracted attention in recent years.¹⁸⁻²⁰ The adsorption performance of AC depends greatly on its well-developed porosity and surface chemical properties. The physicochemical properties of AC are tightly related to its raw materials and the method of preparation. Phosphoric acid activation is a customary method of producing ACs and has become the major method for the industrial preparation of ACs because of its lower activation temperature and less pollution.^{21,22}

To obtain high-performance ACs, phosphoric acid activation doped with oxalic acid (OA) /succinic acid (SA) employed to replace a single activating agent method for the preparation of AC. Since tartaric acid and citric acid have multiple groups that can easily bind on the adsorbent's surface, impregnating tartaric acid and citric acid onto adsorbent (activated carbons and lignocellulose materials) was used to improve their adsorption ability.^{23,24} However, thus far no relevant studies have been performed on modifying activated carbon with OA and SA during the preparation

process. At elevated temperature, phosphoric acid as a good catalyst could promote not only the hydrolysis of lignocelluloses, but also the etherification and esterification between PA and OA/SA.²⁴ Thus, this modification method may increase the acidic groups of the produced activated carbon.

The resource of PA is abundant in the constructed wetland in China. With the harvest of PA in winter in the constructed wetland, great deals of wastes of PA were left. In this work, PA served as raw materials to prepare ACs by phosphoric acid activation doped with the oxalic acid/succinic acid. The modified ACs were the first time used as adsorbent for RhB removal and the adsorption equilibrium and kinetics properties of RhB on ACs were measured.

2. Materials and methods

2.1 Adsorbate and Chemicals

A stock solution of 1000 mgL⁻¹ of RhB was prepared by dissolving 1 g of dye in 1000 ml of double distilled water and used for further studies by diluting as concentrations required. The properties of dye and organic acids (OA and SA) are given in Table S1 and Table S2, respectively. All chemical reagents used in this study were of analytical grade.

2.2. Preparation of activated carbon

Phragmites australis (PA) was harvested from Nansi Lake in Shandong Province (China). PA was washed repeatedly with distilled water to eliminate the dust and

soluble impurities, dried at 105 °C for 12 h and shattered to pieces. PA with a particle size fraction of 0.45-1.0 mm was used as precursor for preparation of activated carbon. PA (10 g) was fully soaked in H₃PO₄ solution (85 wt.%) at the given ratio (g H₃PO₄/g PA) and with different amount of OA/SA (0-0.05 mol). After impregnation at room temperature for 10 h, the samples were heated up to the desired temperature of 450 °C and maintained for 1 h in a muffle furnace under pure N₂ conditions. After cooling to room temperature, carbonized materials were thoroughly washed with distilled water until the pH of the washing liquid was steady. Finally, ACs were filtered, dried at 105 °C for 10 h and sieved to 120 mesh with standard sieves (Model U200).

2.3. Characterization methods

The pore structure characteristics of ACs were determined by N₂ adsorption/desorption at 77 K after degasing at 250 °C for 6 h using a surface area analyzer (Quantachrome Corporation, USA). Boehm's titration method²⁵ was utilized to quantify the amount of acidic functional groups on the surfaces of AC. The determination of pH_{pzc} (point of zero charge) was carried out following a batch method proposed in the literature.²⁶ The surface functional groups of ACs (ACs before and after RhB adsorption) were analyzed with a Fourier transform infrared (FTIR) spectroscopy (VERTEX70 spectrometer, Bruker Corporation, Germany). The surface morphology of the carbons was analyzed by a scanning electron microscope (SEM) (Hitachi 4800, Japan). Surface elemental compositions of the carbons were quantified using an X-ray photoelectron spectrometer (XPS) (Thermo SCIENTIFIC

ESCALAB 250, USA) with Al K alpha (1486.8 eV of photons) irradiation source. All the spectra were calibrated by C 1s peak at 284.8 eV.

2.4. Adsorption experiments

Batch adsorption experiments were performed by adding 30 mg ACs into 50 mL RhB solution (400 mg/L) to investigate the effect of contact times, pHs, and ionic strengths on the adsorption. The samples were shaken at room temperature of 25 ± 1 °C and 120 rpm for 24 h to ensure that sorption equilibrium was reached. Duplicate samples were prepared for all adsorption experiments. After equilibrium, the samples were filtered through a 0.45 µm membrane filters. The initial and residual concentration of RhB was determined by a UV-vis spectrophotometer (UV-5100, Shanghai) at the wavelength of 552 nm. The removal efficiency and the amounts of RhB adsorbed on ACs, Q_e (mg/g), were calculated using the following equation (1) and (2):

$$\text{Removal efficiency (\%)} = \frac{C_0 - C_e}{C_0} \times 100\% \quad (1)$$

$$Q_e = (C_0 - C_e)V/W \quad (2)$$

where C_0 and C_e are the initial and equilibrium concentrations of RhB in the aqueous solution (mg/L), respectively, V is the volume (L) of the solution, and M is the mass of adsorbent used (g).

3. Results and discussion

3.1. Preparations

Effect of impregnation ratio (IR) and duration on the acidic groups and adsorption

equilibrium of RhB were evaluated at the concentration of 400 mg/L and equilibrium time of 12 h (Fig. S1). It can be clearly observed that acidic groups increased from 1.05 to 1.85 with increasing IR from 0.5 to 2.0, and then slightly decreased when IR was higher than 2.0. The maximum concentration was obtained at impregnation ratio of 2.0. The RhB removal efficiency followed the same trend. At low IR, the interactions between activation agent and precursors or the hydrolysis products of precursors resulted in the formation of functional groups which were stable. With the increase of impregnation ratio, the activation agent which was unable to incorporate into the particle of precursors formed a hard film surrounding the particle, prohibiting the diffusion of oxygen into the particle. The trend of RhB removal efficiency was attributed that the acidic groups play a key role in RhB adsorption. From Fig. S1 (b), the best impregnation time at 10 h.

Effect of OA and SA ratios on the removal efficiency of RhB were performed by adding 30 mg ACs into 50 mL 600mg/g RhB solution (Fig. S2). It can be clearly observed that RhB removal efficiency increased 57% to 85% with increasing OA ratio from 0.01 to 0.04 (see Fig. S2 (a)). Beyond the value, further increase in the ratio showed a gradually decrease of RhB removal efficiency. Similarly, SA ratio from 0.01 to 0.04 illustrated an enhancement of RhB removal efficiency increased from 63% to 97% (see Fig. S2 (b)), and then steadily decreased. The best removal efficiency of RhB was obtained at the organic acid/PA ratio of 0.04 mol/10 g PA. From the obtained results, the best removal efficiency of RhB of carbons was used in the further investigation of the physicochemical properties and the factors affecting of on the

adsorption experiments.

3.2. Characterizations.

Fig. 1 shows the SEM micrographs of AC, AC-OA and AC-SA. Comparison of these micrographs shows that the modification does not significantly change the morphology of the surface matrix of the carbons. However, the acid modification reduces the number of cracks and cavities on the carbon surface, which are the more corrosion of OA and SA for carbon surface in activation. N_2 adsorption and desorption isotherms and pore size distributions for ACs are depicted in Fig. 2. It was found that mesoporous structure for each AC was indicated by the presence of hysteresis for each isotherm at P/P_0 above 0.4 (Fig. 2a). The results also can be confirmed by pore size distributions that the carbon had some pores with pore width between 2 and 9 nm (Fig. 2b). The textural parameters of ACs are shown in Table 1. AC-OA and AC-SA possessed the larger surface area and V_{tot} than AC, which mainly due to the doped organic acids increased the corrosion. AC-SA exhibited the highest surface area, V_{mic} and V_{ext} , whereas AC-OA exhibited higher mesoporous structure and higher pore volume than AC.

The results of Boehm's titrations are given in Table 1. AC-OA and AC-SA contained more acidic groups than AC, indicating that organic acid modification obviously enhanced the surface acidity of ACs. Fixation of the acidic groups on the surface of ACs makes it more hydrophilic and decreases its pH of pH_{pzc} . Obvious differences existed between the amounts of acidic functional groups of ACs,

confirming the observed pH_{pzc} existed within acidic range. AC-SA contained notably largest amounts of acidic groups. The amounts of acidic groups on the surfaces of three ACs were as follows: phenolic > carboxylic > lactonic. Fig. 3 shows the C 1s and O 1s peaks of the ACs. It exhibited that the C 1s could be fit to three curves: C-C or C-H at 284.78-284.8 eV; C-O in alcohol, phenol, or ether at 286.34–286.56 eV; and O-C=O or C=O at 288.31-289.15 eV. The O 1s peak could be fitted to three curves: -C=O at 531.15–531.33 eV; C-OH or C-O-C at 532.96-532.99 eV; chemisorbed oxygen (carboxylic groups) and/or water at 535.28-536.03 eV. The fitting parameters of C 1s and O 1s curves are calculated and showed in Table 2. According to Table 1, the acidic groups values of AC, AC-OA and AC-SA are 1.852, 2.987 and 3.194 mmol/g, respectively, which means that modified ACs have more acidic functional groups.

3.2. Adsorption kinetics

Adsorption is a time-dependent process, and it is important to predict the removal rate of contaminants from aqueous solution. Fig. 4 (a) shows the effect of contact time on the RhB adsorption by ACs. The adsorption capacities of RhB onto three carbons increases rapidly in the first 50 min and thereafter gradually increase until it reached equilibrium. The fast adsorption during the initial stage may be due to the fact that higher driving force enabled the fast transfer of RhB to the surfaces of adsorbent particles. After a period of time, the adsorption became difficult because the number of vacant sites decreased and a repulsive force formed between the solute molecules

on the solid surface and in the bulk phase.²⁷ It is worthy to note that the maximum adsorption capacity was achieved within 60 min for all ACs, indicating that the ACs could be desirable adsorbents for wastewater treatment plant applications. Furthermore, it could be observed that the modified ACs (AC-OA and AC-SA) had higher RhB adsorption capacities than the unmodified carbon (AC).

The adsorption kinetics usually are used to describe the solute uptake rate on the adsorbent and the possible mechanism of adsorption. The pseudo-first order²⁸ based on solid capacity is defined as:

$$\ln(Q_e - Q_t) = \ln Q_e - k_1 t \quad (3)$$

The pseudo-second order²⁹ predicts the behavior over the whole range of adsorption and represented by:

$$\frac{t}{Q_t} = \frac{1}{k_2 Q_e^2} + \frac{1}{Q_e} t \quad (4)$$

Elovich kinetic equation³⁰ is one of the most useful models describing chemisorption processes, given by:

$$Q_t = \frac{1}{b} \ln(ab) + \frac{1}{b} \ln t \quad (5)$$

where Q_e and Q_t (mg/g) are the amount of RhB adsorbed on the adsorbents at equilibrium and at time t , respectively; k_1 (1/min) and k_2 (mg min) is the pseudo-first-order and pseudo-second-order rate constant; a (mg/g h) is the initial sorption rate and b (g/mg) is related to the extent of surface coverage and activation energy for chemisorption. Table 3 shows the parameters of pseudo-first-order, pseudo-second-order and Elovich kinetic models for the adsorption of RhB onto ACs. Obviously, pseudo-second order model yielded the best fit, with highest correlation

coefficients ($R^2 > 0.99$). This suggested that the overall rate of the adsorption process was controlled by chemisorption which involved valency forces through electrons sharing between the adsorbent and adsorbate. Accordingly, it was found that the internal and external surfaces of the porous carbons were easily accessible for RhB.

As the above kinetic models were not able to identify the diffusion mechanism, thus intra-particle diffusion model³¹ found functional relationship, common to the most adsorption processes. According to this theory:

$$Q_t = k_{pi}t^{1/2} + C_i \quad (6)$$

where k_{pi} ($\text{mg}/(\text{g min}^{1/2})$) is the diffusion rate constant of intra-particle, C_i gives an idea about the thickness of boundary layer. Fig. 4 (b) shows the intra-particle plot for RhB onto ACs. It was evident that the adsorption process follows three steps, which indicates a multi-stage adsorption processes. The diffusion parameters of each region are shown in Table 3. Each step can be identified by a change in the slope of the linear line, which is used to fit the experimental data. These results could be illustrated as follows: the first region was very sharp and indicated rapid attachment of RhB molecules to the external surface of ACs. The second linear region was the gradual adsorption stage in which the intra-particle diffusion was the rate-limiting step. The third region showed the final equilibrium stage where RhB diffusion was very slow due to its low concentration. It can be seen that the linear lines of the second and the third stage did not pass through the origin. Therefore, intra-particle diffusion was not the only rate limiting-step and chemisorption or physisorption may be involved in the process.²⁷

3.3. Adsorption isotherms

The equilibrium isotherms in this study were analyzed using the Langmuir, Freundlich and Temkin isotherms. The Langmuir isotherm theory³² assumes monolayer coverage of adsorbate over a homogenous adsorbent surface and represented by:

$$\frac{C_e}{q_e} = \frac{1}{q_m k_L} + \frac{1}{q_m} C_e \quad (7)$$

The Freundlich isotherm³³ is an empirical equation assuming that the adsorption process takes place on heterogeneous surfaces and given by:

$$\log q_e = \log K_F + \left(\frac{1}{n}\right) \log C_e \quad (8)$$

Temkin and Pyzhev considered the effects of some indirect adsorbate/adsorbate interactions on adsorption isotherms and suggested that because of these interactions the heat of adsorption of all the molecules in the layer would decrease linearly with coverage¹. The Temkin isotherm has been used in the following form:

$$q_e = \left(\frac{RT}{b}\right) \ln A + \left(\frac{RT}{b}\right) \ln C_e \quad (9)$$

$$B = \frac{RT}{b} \quad (10)$$

where q_e (mg/g) is the amount of RhB adsorbed by ACs at equilibrium; C_e (mg/L) is the equilibrium concentration of RhB; q_m is the maximum amount of RhB that form a complete monolayer on the adsorbents surface; k_L is adsorption equilibrium constant (L/mg). k_F ($\text{mg}^{1-1/n} \text{L}^{1/n}/\text{g}$) and n are Freundlich constant, representing the adsorption capacity of the adsorbent and adsorption intensity, respectively. A (l/g) and B are Temkin constants. The relative parameters calculated from the isotherm models are shown in Table 4. The adsorption isotherms for ACs along with the non-linear fit of

experimental data are presented in Fig. 5. The Langmuir model fitted the data better than the Freundlich and Temkin model with higher R^2 , implying that RhB adsorption on ACs was a monolayer adsorption and uniform adsorptions. The observed k_L values shows that the adsorbent prefers to bind acidic ions and that speciation predominates on sorbent characteristics, when ion exchange is the predominant mechanism takes place in the adsorption of RhB. Li et al. also reported the sorption of RhB onto carbon prepared from scrap tires, in which the equilibrium experimental data were better fitted to a Langmuir isotherm.³⁴

3.4. Effect of initial pH and ion strengthens

Solution pH would affect both aqueous chemistry and surface binding-sites of the adsorbent. The effect of pH on the adsorption of RhB by ACs is presented in Fig. 6 a and b. The effect of pH on RhB removal was studied by adjusting initial pH from 2.0 to 12.0 with 0.1 M HCl or NaOH. The pH values of solutions after the sorption experiments are shown in Fig. 6 a. The final equilibrium pH values became lower after the adsorption of RhB. Furthermore, the final pH values of AC-OA and AC-SA were lower than that of AC. One possible reason maybe that the acidic functional groups on the surface of ACs releasing H^+ into the solution. A similar phenomenon has been reported by Zhang et al.,¹³ in which the presence of acidic functional groups on the surface was likely to give considerable cation exchange capacity to the adsorbents.

The equilibrium RhB adsorption capacities of ACs in different pH ranges (Fig.

6 b) was first increased from initial pH 2 to 4, reached approximate maximum at the initial pH 4. Then, reduced tardily from initial pH 4 to 10, while decreased sharply over initial pH 10. The influence of pH on the pronounced sorption of RhB on the surface of ACs at low pH ranges leads to the assumption that chemisorptions dominates in this range and chemisorptions along with physisorption occurs at higher pH ranges¹³. In addition, it appears that a change in pH of the solution results in the formation of different ionic species ($pK_a=3.7$),³⁵ and different carbon surface charge. At pH values lower than 4, RhB ions are of cationic and monomeric molecular form. Thus RhB can enter into the pore structure. At a pH value 4-10, the zwitterionic form of RhB in water may increase the aggregation of RhB to form a larger molecular form (dimer) and become unable to enter into the pore. At a pH value higher than 10, the OH⁻ neutralized the surface acidic functional groups of ACs.^{13,36}

Dye containing wastewater often contains various salts, which lead to high ionic strength and may affect the dye adsorption onto adsorbents. The adsorption experiments to evaluate the ionic strength effect were carried out by adding NaCl at different concentrations (0-500 mmol/L). As showed in Fig. 6c, the amount of RhB absorbed showed only a tiny change in the increasing NaCl concentrations. This attributed that adsorption of RhB by ACs were unacted on ions strengthen.

3.5. Adsorption mechanism and capacities

Surface functional groups of AC, AC-OA and AC-SA were investigated by using FTIR spectroscopy in the ranges of 400-4000 cm^{-1} (Fig. 7 a). After RhB adsorption,

the functional groups of ACs were also measured and compared (Fig. 7 c). The forms of bands for the three types of ACs were very similar, indicating that ACs have similar functional groups. However, the transmittances of modified carbons (AC-OA and AC-SA) were larger than that of AC, attributing that the amounts of modified carbons were more than that of AC. The bands at 3435 and 1715 cm^{-1} represented the stretching frequency of the hydroxyl group and carboxylic group. The peaks at 1625 cm^{-1} may be attributed to the stretching frequency of the asymmetric stretching vibration of $-\text{COO}$, the bands at 1170 and 671 cm^{-1} correspond to C-O and C-H stretching vibration. After the adsorption of RhB, some new absorption bands occurred on dye-loaded activated carbons (Fig. 4 c), which due to the pore-filling of adsorbent. The swings of bands at 3435, 1715, 1625 1170 and 671 cm^{-1} were smaller than that of before adsorption of RhB, implying that the acidic functional groups could adsorb more RhB species by electrostatic attraction, cation exchange and surface complexation.

From Table 1, the S_{BET} and V_{tot} of AC-OA and AC-SA were higher than those of AC, meanwhile modified carbons showed more acidic groups, attributing that the RhB adsorption capacities of AC-OA and AC-SA were much more than that of AC. However, compared to the porosity, acidity and adsorption capacities of AC, AC-OA and AC-SA. It could be concluded that surface functionality rather than pore structure plays a more crucial role in determining the adsorption capacity of RhB.

Table 5 shows the comparison of the maximum adsorption capacities of RhB onto various adsorbents. Although the published values were obtained under different

experimental conditions, they may be useful as a criterion for comparing the adsorption capacities. It can be seen that the RhB adsorption capacities of ACs in this study were ultrahigh and larger than other carbon adsorbents.

4. Conclusion

In this work, Oxalic acid and succinic acid were employed to modify PA-based ACs during phosphoric acid activation for improving its Rhodamin B removal from aqueous solutions. The prepared ACs exhibited high specific surface area, porosity and acidity. The adsorption capacities are ultrahigh and significantly influenced by the contact time and pH value. Adsorption kinetics were found to follow the pseudo-second order kinetic model for the activated carbons. The adsorption equilibrium data were better fitted to the Langmuir model.

Acknowledgements

This work was supported by the Independent Innovation Foundation of Shandong University (2012JC029), Natural Science Foundation for Distinguished Young Scholars of Shandong Province (JQ201216) and National Water Special Project (2012ZX07203-004).

Reference

1. B. Hameed, *Journal of hazardous materials*, 2009, 161, 753-759.
2. Y. Wong and J. Yu, *Water Research*, 1999, 33, 3512-3520.
3. K. Kadirvelu, C. Karthika, N. Vennilamani and S. Patabhi, *Chemosphere*, 2005, 60, 1009-1017.

4. S.-H. Chang, K.-S. Wang, H.-C. Li, M.-Y. Wey and J.-D. Chou, *Journal of hazardous materials*, 2009, 172, 1131-1136.
5. L. Peng, P. Qin, M. Lei, Q. Zeng, H. Song, J. Yang, J. Shao, B. Liao and J. Gu, *Journal of hazardous materials*, 2012, 209, 193-198.
6. R. Jain, M. Mathur, S. Sikarwar and A. Mittal, *Journal of Environmental Management*, 2007, 85, 956-964.
7. J.-H. Huang, K.-L. Huang, S.-Q. Liu, A.-T. Wang and C. Yan, *Colloids and Surfaces A: Physicochemical and Engineering Aspects*, 2008, 330, 55-61.
8. K. P. Singh, S. Gupta, A. K. Singh and S. Sinha, *Chemical Engineering Journal*, 2010, 165, 151-160.
9. L. Fan, Y. Zhou, W. Yang, G. Chen and F. Yang, *Dyes and Pigments*, 2008, 76, 440-446.
10. Y. Anjaneyulu, N. S. Chary and D. S. S. Raj, *Reviews in Environmental Science and Bio/Technology*, 2005, 4, 245-273.
11. K. Kadirvelu, M. Kavipriya, C. Karthika, M. Radhika, N. Vennilamani and S. Pattabhi, *Bioresource technology*, 2003, 87, 129-132.
12. H. Zhong, Y. Shaogui, J. Yongming and S. Cheng, *Journal of Environmental Sciences*, 2009, 21, 268-272.
13. H. M. Gad and A. A. El-Sayed, *Journal of hazardous materials*, 2009, 168, 1070-1081.
14. Z. Guo, X. Bian, J. Zhang, H. Liu, C. Cheng, C. Zhang and J. Wang, *Journal of the Taiwan Institute of Chemical Engineers*, 2014, 45, 2801-2804.
15. Z. Guo, J. Fan, J. Zhang, Y. Kang, H. Liu, L. Jiang and C. Zhang, *Journal of the Taiwan Institute of Chemical Engineers*, 2015.
16. P. Chingombe, B. Saha and R. Wakeman, *Carbon*, 2005, 43, 3132-3143.
17. R. Reit, J. Nguyen and W. J. Ready, *Electrochimica Acta*, 2013, 91, 96-100.
18. H. Liu, J. Zhang, W. Liu, N. Bao, C. Cheng and C. Zhang, *Materials Letters*, 2012, 87, 17-19.
19. H. Liu, X. Wang, G. Zhai, J. Zhang, C. Zhang, N. Bao and C. Cheng, *Chemical Engineering Journal*, 2012, 209, 155-162.
20. Y. Wang, H. Ngo and W. Guo, *Science of The Total Environment*, 2015, 533, 32-39.
21. J. Laine and A. Calafat, *Carbon*, 1989, 27, 191-195.
22. H. Teng, T.-S. Yeh and L.-Y. Hsu, *Carbon*, 1998, 36, 1387-1395.
23. K. Sreejalekshmi, K. A. Krishnan and T. Anirudhan, *Journal of Hazardous Materials*, 2009, 161, 1506-1513.
24. H. Liu, S. Liang, J. Gao, H. H. Ngo, W. Guo, Z. Guo, J. Wang and Y. Li, *Chemical Engineering Journal*, 2014, 246, 168-174.
25. H. Boehm, *Carbon*, 1994, 32, 759-769.
26. B. Babić, S. Milonjić, M. Polovina and B. Kaludierović, *Carbon*, 1999, 37, 477-481.
27. G. Zhang, L. Shi, Y. Zhang, D. Wei, T. Yan, Q. Wei and B. Du, *RSC Advances*, 2015, 5, 25279-25286.
28. W. J. Weber and J. C. Morris, *Journal of the Sanitary Engineering Division*, 1963, 89, 31-60.
29. Y.-S. Ho and G. McKay, *Process biochemistry*, 1999, 34, 451-465.
30. C. Aharoni and F. Tompkins, *Advances in catalysis and related subjects*, 1970, 21, 1-49.
31. Z. Guo, L. Xu, C. Liu, F. Sun, Y. Kang and S. Liang, *Desalination and Water Treatment*, 2015, 1-11.
32. I. Langmuir, *Journal of the American Chemical society*, 1918, 40, 1361-1403.

33. H. Freundlich, *J. Phys. Chem*, 1906, 57, e470.
34. L. Li, S. Liu and T. Zhu, *Journal of Environmental Sciences*, 2010, 22, 1273-1280.
35. S. Merouani, O. Hamdaoui, F. Saoudi and M. Chiha, *Chemical Engineering Journal*, 2010, 158, 550-557.
36. B. Hameed, *Journal of hazardous materials*, 2008, 154, 204-212.
37. Y. Guo, J. Zhao, H. Zhang, S. Yang, J. Qi, Z. Wang and H. Xu, *Dyes and Pigments*, 2005, 66, 123-128.
38. J. Anandkumar and B. Mandal, *Journal of hazardous materials*, 2011, 186, 1088-1096.
39. L. Wang, J. Zhang, R. Zhao, C. Li, Y. Li and C. Zhang, *Desalination*, 2010, 254, 68-74.
40. L. Ding, B. Zou, W. Gao, Q. Liu, Z. Wang, Y. Guo, X. Wang and Y. Liu, *Colloids and Surfaces A: Physicochemical and Engineering Aspects*, 2014, 446, 1-7.

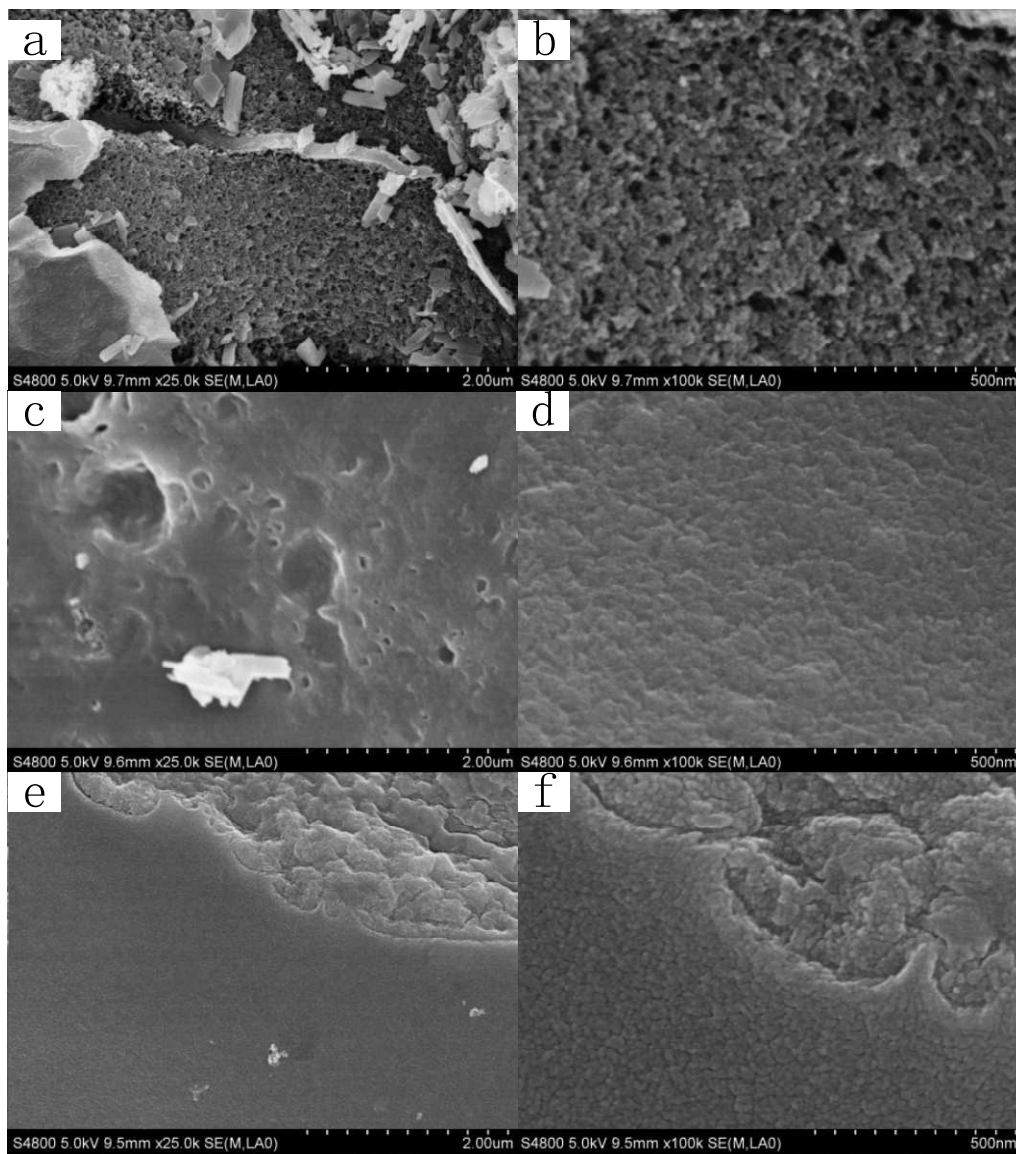


Fig. 1 SEM images of AC (a and b), AC-OA (c and d) and AC-SA (e and f) (a, c and e, magnification 25,000 \times ; b, d and f, magnification 100,000 \times).

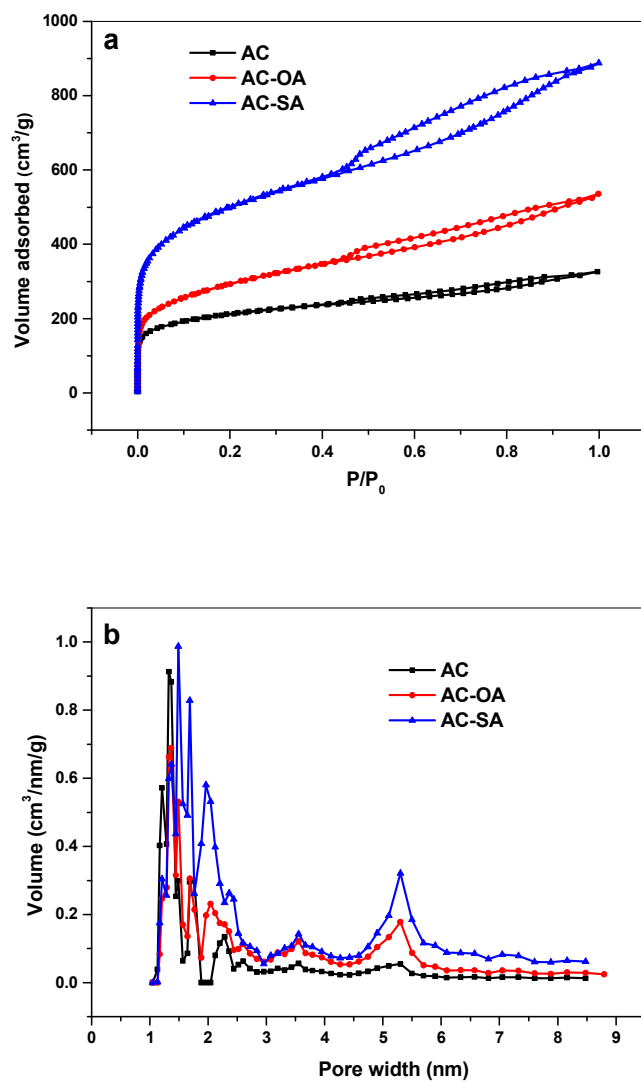


Fig. 2 (a) N_2 adsorption and desorption isotherms and (b) pore size distributions of activated carbons.

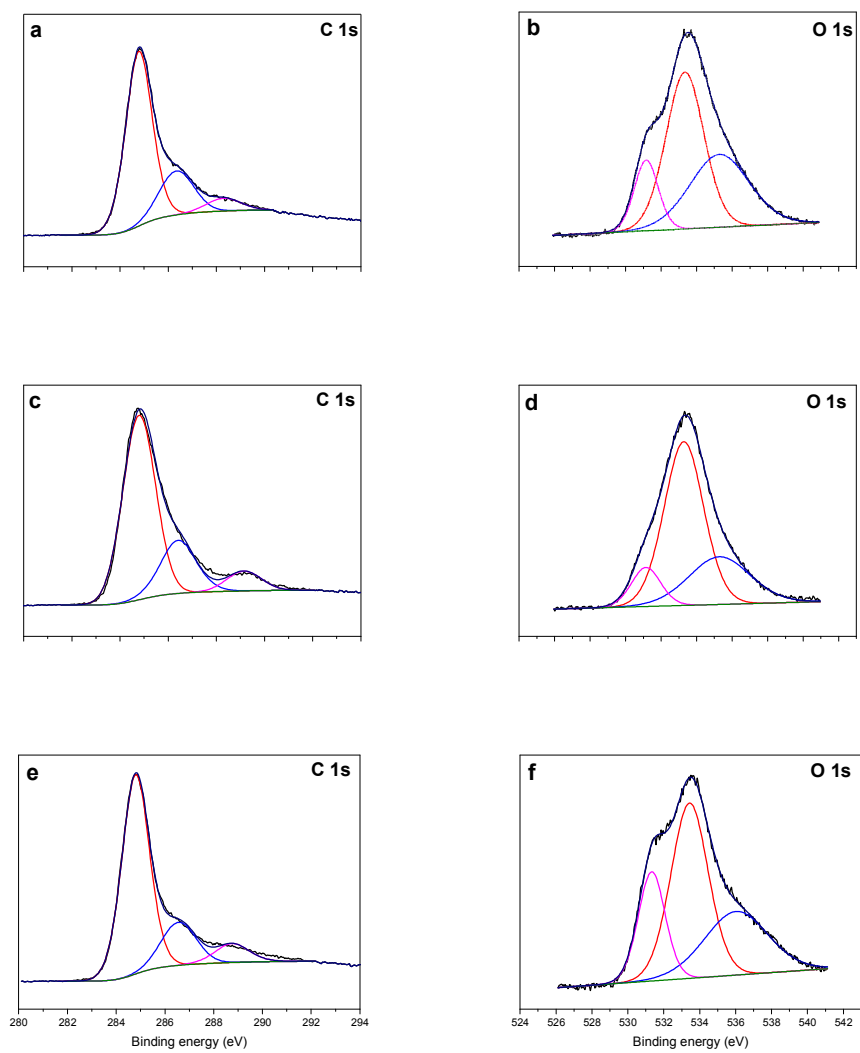


Fig. 3. C 1s and O 1s XPS spectra of AC (a and b), AC-OA (c and d) and AC-SA (e and f).

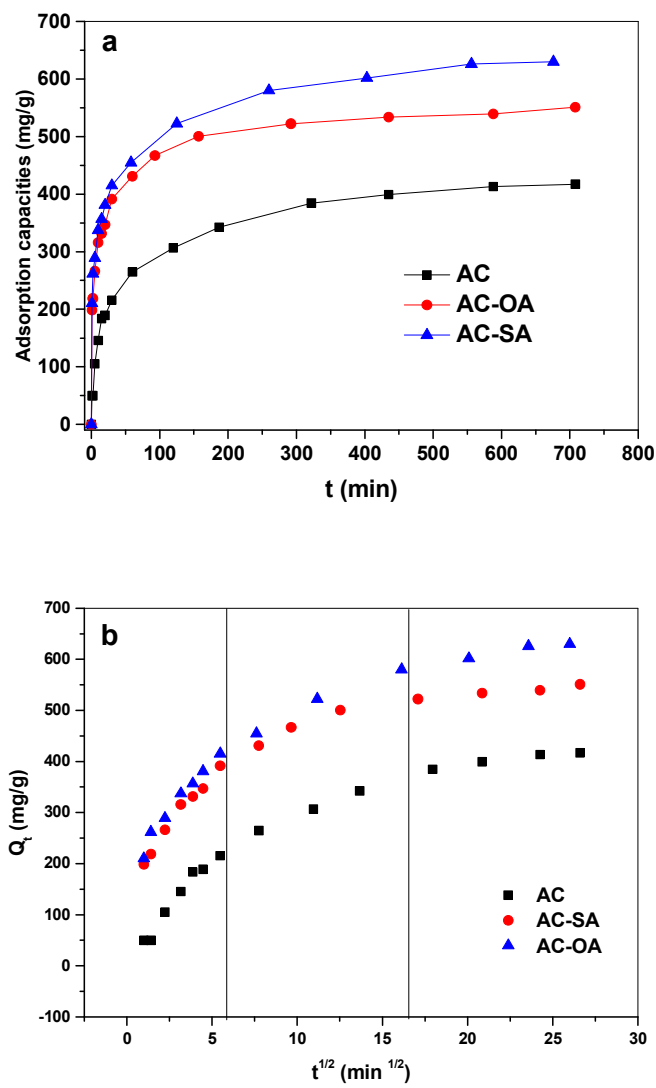


Fig. 4 (a) Effect of contact time of RhB adsorption on AC, AC-OA, and AC-SA, (b) intra-particle diffusion plots for RhB onto activated carbons (Dosage = 0.6 g L⁻¹, temperature = 25 ± 1 °C, initial pH = 4.00 ± 1, time = 12 h).

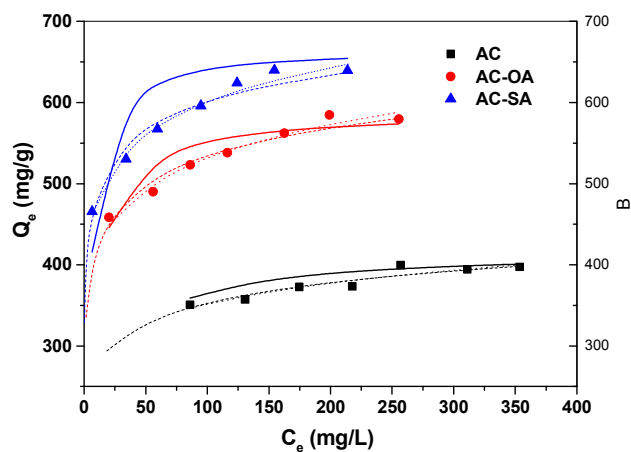


Fig. 5 Adsorption isotherms of RhB onto activated carbons. Solid lines represent the Langmuir isotherms, dash lines represent the Freundlich isotherms and dot line represent the Temkin isotherms. (Dosage = 0.6 g L⁻¹, temperature = 25 ± 1 oC, initial pH = 4.00 ± 1, time = 12 h).

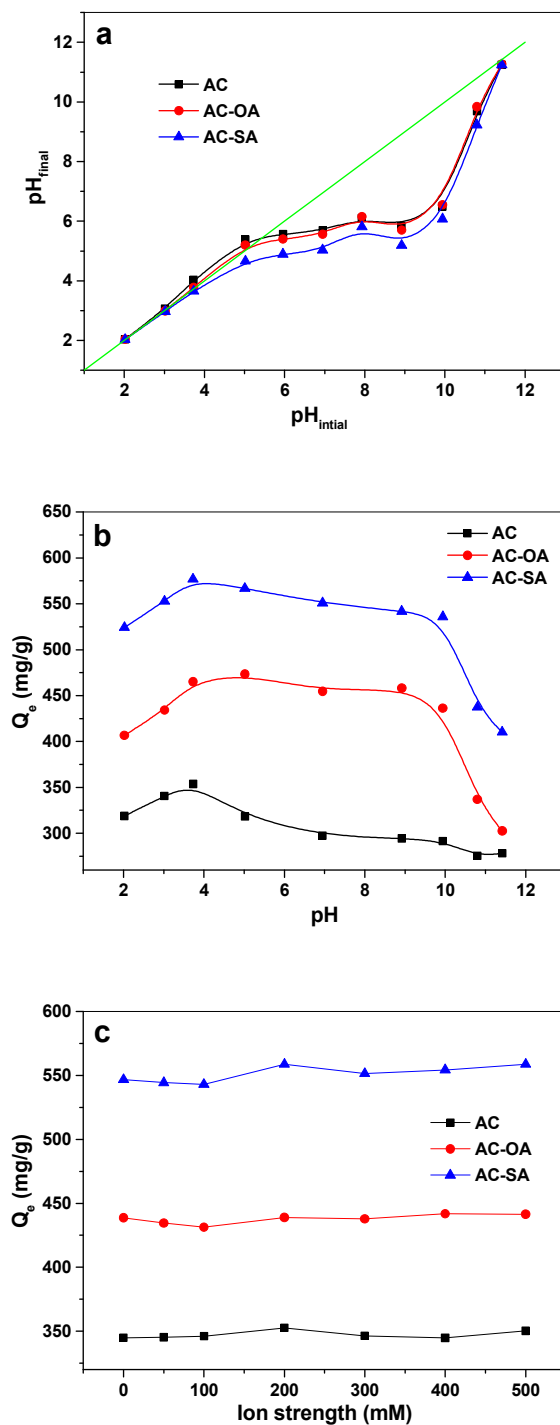


Fig. 6. (a) The change of pH values after adsorption of RhB, (b) RhB adsorption capacities by the carbons in different pH ranges and (c) effect of ionic strengths (NaCl) on RhB adsorption. (Dosage = 0.6 g L^{-1} , temperature = $25 \pm 1 \text{ }^\circ\text{C}$, time = 12 h)

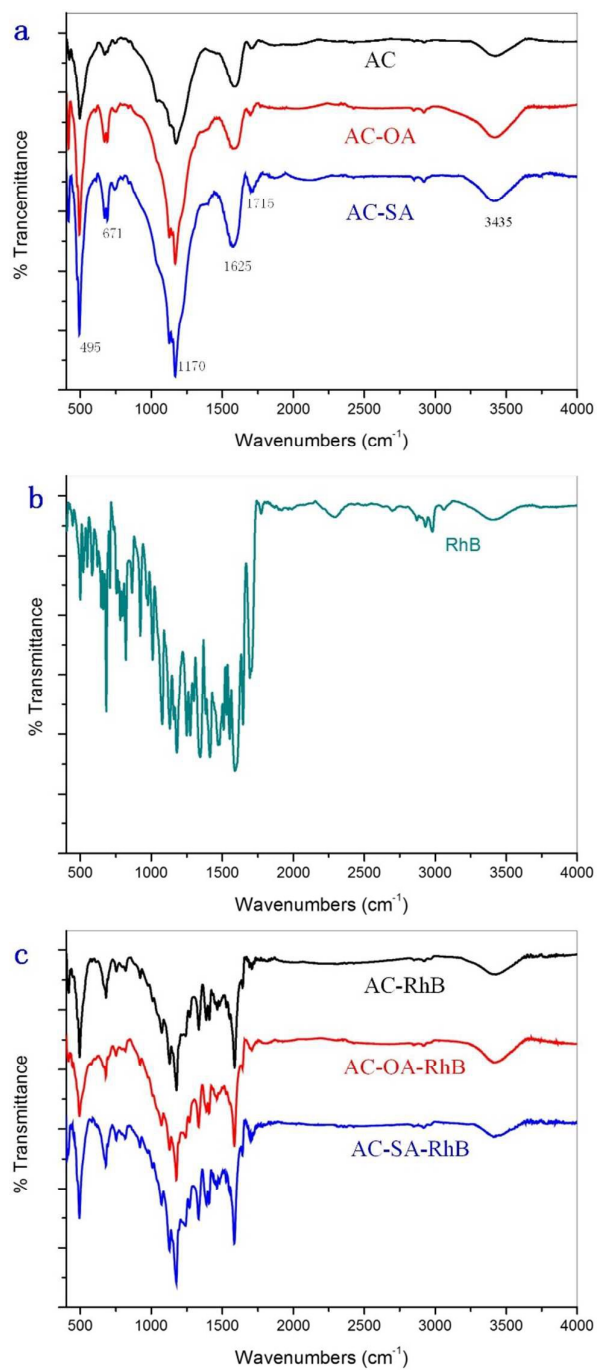


Fig. 7. (a) The infrared spectra of activated carbons, (b) the infrared spectra of RhB

and (c) the infrared spectra of activated carbons after adsorption of RhB.

Table 1. Textural and chemical characteristics of activated carbons

| Activated carbon | AC | AC-OA | AC-SA |
|---|--------|---------|---------|
| S_{BET}^a (m ² g ⁻¹) | 745.68 | 1040.36 | 1775.01 |
| S_{mic}^b (m ² g ⁻¹) | 489.35 | 471.16 | 953.42 |
| S_{ext}^c (m ² g ⁻¹) | 256.33 | 569.20 | 821.58 |
| V_{mic}^d (cm ³ g ⁻¹) | 0.221 | 0.213 | 0.426 |
| V_{ext}^e (cm ³ g ⁻¹) | 0.200 | 0.465 | 0.736 |
| V_{tot}^f (cm ³ g ⁻¹) | 0.421 | 0.678 | 1.162 |
| Carboxylic groups g (mmol g ⁻¹) | 0.793 | 1.098 | 1.205 |
| Lactonic groups g (mmol g ⁻¹) | 0.235 | 0.127 | 0.206 |
| Phenolic groups g (mmol g ⁻¹) | 0.824 | 1.762 | 1.783 |
| Total acidity g (mmol g ⁻¹) | 1.852 | 2.987 | 3.194 |
| pH _{pzc} h | 4.01 | 3.50 | 3.15 |

^a BET surface area (S_{BET}) was determined by using the Brunauer-Emmett-Teller (BET) theory. ^b Micropore surface area (S_{mic}), ^c external surface area (S_{ext}) and ^d micropore volume (V_{mic}) were evaluated by the *t*-plot method. ^e Total pore volume (V_{tot}) was determined from the amount of N₂ adsorbed at a P/P₀ around 0.95. ^f Total pore volume (V_{tot}) was determined from the amount of N₂ adsorbed at a P/P₀ around 0.95. ^g Boehm's titration. ^h pH_{pzc}: point of zero charge.

Table 2 Peak numbers and relative content of the surface functional groups

determined by C 1s and O 1s spectra from XPS for samples.

| Samples | Peak from C 1s spectrum | | | Peak from O 1s spectrum | | |
|---------|-------------------------|--------|--------|-------------------------|---------|----------|
| | Peak 1 | Peak 2 | Peak 3 | Peak I | Peak II | Peak III |
| AC | | | | | | |
| BE (eV) | 284.78 | 286.34 | 288.31 | 531.18 | 533.37 | 535.31 |
| RC (%) | 46.74 | 14.98 | 4.34 | 14.21 | 49.77 | 36.02 |
| AC-OA | | | | | | |
| BE (eV) | 284.79 | 286.41 | 289.15 | 531.15 | 533.28 | 535.28 |
| RC (%) | 51.28 | 16.36 | 5.77 | 10.88 | 61.39 | 27.73 |
| AC-SA | | | | | | |
| BE (eV) | 284.8 | 286.56 | 288.75 | 531.33 | 533.45 | 536.03 |
| RC (%) | 54.95 | 14.48 | 6.35 | 21.76 | 48.40 | 29.84 |

Table 3. Parameters of kinetics models and intra-particle diffusion model for the adsorption of RhB onto activated carbons.

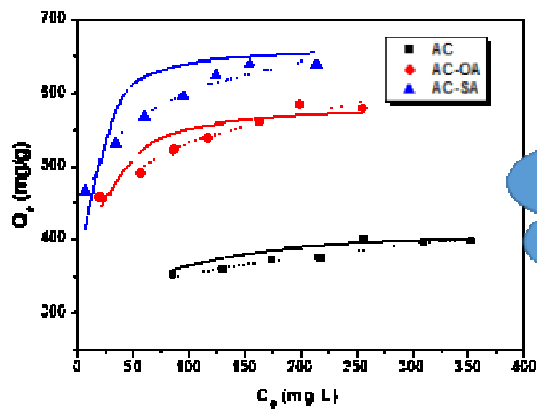
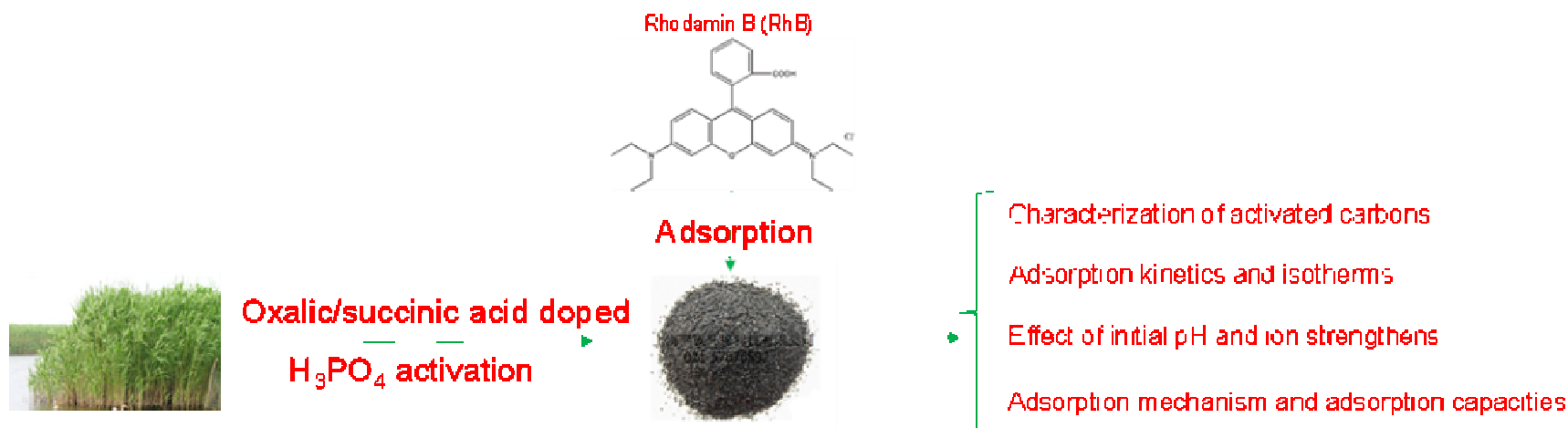
| Kinetic models | parameter | Activated carbons | | |
|-------------------------------------|--|-------------------|---------|---------|
| | | AC | AC-OA | AC-SA |
| Pseudo-first-order parameters | $Q_{e,exp}$ (mg/g) | 417.1 | 550.9 | 629.8 |
| | $Q_{e,cal}$ (mg/g) | 287.5 | 247.4 | 331.7 |
| | K_1 (1/min) | 0.0048 | 0.0046 | 0.005 |
| | R^2 | 0.9570 | 0.8755 | 0.9443 |
| Pseudo-second-order parameters | $Q_{e,cal}$ (mg/g) | 434.8 | 500.0 | 526.3 |
| | K_2 (g mg ⁻¹ min ⁻¹ 10 ⁻⁴) | 0.8802 | 1.754 | 1.249 |
| | R^2 | 0.9975 | 0.9991 | 0.9978 |
| Elovich kinetic parameters | a | 80.05 | 1445.92 | 1193.85 |
| | b | 0.016 | 0.017 | 0.015 |
| Intra-particle diffusion parameters | $Q_{e,cal}$ (mg/g) | 420.36 | 565.17 | 617.44 |
| | R^2 | 0.9911 | 0.9890 | 0.9919 |
| | K_{p1} (mg g ⁻¹ min ^{-1/2}) | 44.807 | 54.83 | 43.012 |
| | C_1 | 0.0738 | 142.73 | 188.67 |
| | $(R_1)^2$ | 0.9851 | 0.9995 | 0.9719 |
| | K_{p2} (mg g ⁻¹ min ^{-1/2}) | 15.095 | 23.173 | 14.529 |
| | C_2 | 139.48 | 248.93 | 349.94 |
| | $(R_2)^2$ | 0.9860 | 0.9718 | 0.9805 |
| | K_{p3} (mg g ⁻¹ min ^{-1/2}) | 3.8467 | 3.3717 | 5.3155 |
| | C_3 | 317.27 | 460.93 | 495.38 |
| | $(R_3)^2$ | 0.9700 | 0.9734 | 0.9736 |

Table 4. Langmuir, Freundlich and Temkin isotherm constants for RhB adsorption onto activated carbons.

| Isotherm models | Constants | Activated carbons | | |
|-----------------|--|-------------------|--------|--------|
| | | AC | AC-OA | AC-SA |
| Langmuir | K_L (L mg ⁻¹) | 0.0745 | 0.1545 | 0.2542 |
| | q_m (mg g ⁻¹) | 417.3 | 550.2 | 629.7 |
| | R^2 | 0.9981 | 0.9980 | 0.9982 |
| Freundlich | K_F (mg g ⁻¹ (L mg ⁻¹) ^{1/n}) | 220.6 | 326.4 | 386.1 |
| | $1/n$ | 0.1014 | 0.1063 | 0.0963 |
| | R^2 | 0.9770 | 0.9834 | 0.9862 |
| Temkin | A (L/g) | 226.32 | 595.33 | 4074.8 |
| | B | 35.275 | 48.664 | 46.58 |
| | R^2 | 0.9697 | 0.9887 | 0.9862 |

Table 5. Comparison of the maximum adsorption capacities of RhB onto various adsorbents.

| Adsorbents | Q_{\max} (mg/g) | Reference |
|--|-------------------|-----------|
| AC | 417.1 | This work |
| AC-OA | 550.9 | This work |
| AC-SA | 629.8 | This work |
| Sago waste carbon | 16.2 | 3 |
| Scrap tires activated carbon | 307.2 | 34 |
| Bagasse pith activated carbon | 263.85 | 13 |
| Rice husk-based porous carbon | 431.1 | 37 |
| Modified tannery waste | 250.1 | 38 |
| <i>P.orientale</i> Linn activated carbon | 560.0 | 39 |
| Rice husk-based activated carbon | 400.8 | 40 |



Maximum adsorption capacity reached 629.8 mg/g